Demmel, F., Seydel, T., Jahn, S. (2009): Sodium diffusion in cryolite at elevated temperatures studied by quasielastic neutron scattering. - Solid State Ionics, 180, 23-25, 1257-1260

DOI: 10.1016/j.ssi.2009.07.005

Sodium diffusion in cryolite at elevated temperatures studied by quasielastic neutron scattering

Franz Demmel

ISIS Facility, Didcot, OX11 0QX, United Kingdom

Tilo Seydel

Institute Laue-Langevin, BP 156, 38042 Grenoble Cedex 9, France

Sandro Jahn

Deutsches GeoForschungsZentrum GFZ, Section 3.3, Telegrafenberg, 14473 Potsdam, Germany

Abstract

Quasielastic neutron scattering (QENS) has been applied to study the sodium mobility on nanosecond time scales in the perovskite fluoride cryolite, Na_3AlF_6, at high temperatures. Up to $T = 1153$ K the diffusion of Na ions is well described by a diffusion process of jumps between six and eight fold coordinated sites. Above this temperature, where a step-like increase in the electrical conductivity occurs, the jump length increases, which indicates additional jumps over larger distances. The electrical conductivity derived from the self-diffusion coefficient via the Nernst-Einstein relation and the corresponding activation energy are in excellent agreement with the previous conductivity measurements. We conclude that the jump diffusion of sodium ions is the dominant mechanism for the electrical conductivity in cryolite at high temperatures up to $T = 1153$ K.

Key words: Cryolite; Na_3AlF_6; Quasielastic neutron scattering; Ionic conduction; Self-diffusion

* Corresponding author.
Email address: franz.demmel@stfc.ac.uk (Franz Demmel).

Introduction

Materials with perovskite structure that exhibit high ionic conduction at elevated temperatures have been studied extensively due to their potential applications e.g. as solid electrolytes in fuel cells or in solid state batteries (for a recent review see [1]). Fluorite perovskites have been used as analogue material for magnesium silicate perovskite, $MgSiO_3$, which is considered the major phase of the Earth's lower mantle [2–5]. Using complementary experimental techniques, such as electrical conductivity measurements, nuclear magnetic resonance (NMR) spectroscopy, diffraction or quasielastic neutron scattering, and molecular dynamics simulations, diffusion mechanisms in these materials have been investigated and discussed, sometimes with contradictory results [1].

One interesting class of compounds are mixed cation perovskites with stoichiometry $A_2BB'X_6$. An important representative of this structure is the mineral cryolite, Na_3AlF_6 (or Na_2NaAlF_6), that is used in industry as a flux to extract aluminum metal from bauxite. Cryolite has a double perovskite structure with aluminum and sodium ions occupying the center of alternating $[AlF_6]$ and $[NaF_6]$ octahedra. All of the Al^{3+} and one third of the Na^+ cations are six-fold coordinated (Na^{VI}), whereas the remaining Na^+ ions are eight-fold coordinated (Na^{VIII}). At low temperatures, cryolite has a monoclinic crystal structure due to a tilt of the octahedra. Several high temperature x-ray diffraction experiments showed a transition from the monoclinic to a cubic [6,7] or orthorhombic [8] structure around $T = 840$ K. This phase transition is accompanied by a sudden increase in the electrical conductivity. A second jump in the conductivity is observed at $T = 1153$ K, well below the melting point ($T_m = 1280$ K) [9].

For cryolite, diffusion rates can be obtained from NMR spectroscopy since all three nuclei have good NMR properties. At low temperatures, far below the first transition, NMR studies confirmed Na^+ exchange between the six and eight fold coordinated site in the kHz frequency range [10,11]. At $T = 880$ K, which is in the stability field of the cubic phase, the two sites are indistinguishable on the time scale of NMR. Molecular dynamics simulations provide insight into the dynamics on much shorter time scale up to nanoseconds. Whereas Na diffusion in stoichiometric cryolite was not observed in the simulations below $T = 1170$ K, this temperature is considerably reduced when defects (vacancies) are present [12]. This is also consistent with thermodynamic data that suggest non-stoichiometric cryolite at elevated temperatures [13].

Recently we performed a quasielastic neutron scattering (QENS) study on cryolite using a time of flight spectrometer [14]. This technique covers a time scale similar to that of the molecular dynamics simulations. The data analysis

revealed two dynamic processes below and above the transition at $T = 1153$ K: one slow process which was attributed to sodium ion diffusion and a faster second one which might be related to rotational and/or translational motions. The slow process was only a fraction of the energy resolution (30 μeV) and a profound analysis of the involved jump process was not possible. The present study is dedicated to a detailed study of the sodium diffusion processes at temperatures well above the monoclinic to cubic phase transition. In addition to the more precise determination of the Na self-diffusion coefficient by using a high resolution backscattering spectrometer, we apply a jump diffusion model to reveal the geometry of the jump process from the QENS data.

Experimental Details

The synthetic sample was of 99.995 % purity (Testbourne Limited). The powder sample was enclosed in a molybdenum cylindrical container with a wall thickness of 0.2 mm and an inner diameter of 8 mm. After filling the container in inert atmosphere it was sealed by electron beam welding. The same sample has been used before in the low energy resolution experiment [14].

Quasielastic neutron scattering experiments were undertaken at the cold neutron backscattering spectrometer IN16 [15] of the Institute Laue-Langevin (ILL) Grenoble, France. The instrument achieves a very high energy resolution by using backscattering from silicon (111) wafers. Inelastic data were recorded by mechanically Doppler-shifting the incident energy with a Doppler frequency of 14 Hz, which gives an energy transfer range between -14.5 μeV and 14.5 μeV. Spectra were taken at various temperatures between room temperature up to $T = 1233$ K. During heating/cooling periods elastic scans were recorded. Within elastic scans the Doppler drive is on rest and the elastically scattered intensity is recorded. These scans indicate changes in the sample dynamics when processes become faster than the slowest relaxation rate detectable within the resolution of the instrument, i.e. faster than a few nanoseconds. With an elastic wavelength of 6.271 Å the 22 detectors cover a momentum transfer range from 0.1 to 1.9 $Å^{-1}$. The energy resolution of 0.95 μeV (FWHM) was deduced from a vanadium scan. The detectors which cover the small angles have a slightly larger energy resolution of about 1.2 μeV.

For background subtraction and data normalization, spectra of an empty container and a vanadium spiral with dimensions and scattering power similar to the sample were taken, respectively. Corrections to the raw data include subtraction of the background, corrections for the self-absorption of the sample and detector efficiency. Contributions from multiple scattering, intensity from multiphonon scattering and possible fast orientational motions, which are all much broader than the dynamic range of the instrument, are accounted for

by a flat background in the fitting procedure. The fitting procedure took into account different energy resolutions for different detectors. A model function was convoluted with the Gaussian resolution function and fitted to the data.

Results and Discussion

Fig. 1 shows the results from elastic scans at a mean Q-vector of $Q = 0.65$ Å^{-1}. A drastic change in dynamics on the time scale of the instrument, which is about 1 ns, occurs above the monoclinic/cubic transition at $T = 840$ K. Above this temperature, the elastic intensity decreases monotonically with temperature and does not change considerably at the second step of the electrical conductivity increase around $T = 1153$ K. The decrease in intensity is related to the set-in of dynamics on the time scale of the instrument. The small change of elastically scattered intensity at 1153 K indicates that processes with much faster dynamics are mainly responsible for the corresponding jump in conductivity, which we observed in our previous experiment. We related this transition to translational fluorine movements on a 10 ps time scale [14]. Below $T = 840$ K a small decrease in intensity can be observed probably due to the Debye-Waller factor.

In the inset of Fig. 1 the integrated intensity is shown, which represents the total static structure factor, $S(Q)$. It is quite flat, an indication of incoherent scattering. As only sodium has a sizeable incoherent scattering cross section in this compound we observe in this Q-range the sodium movements. Around $Q = 1.4$ Å^{-1} a powder line of cryolite from coherent scattering appears.

To describe the movements quantitatively the following model has been fitted to the spectra:

$$S(Q,\omega) = A(Q)\delta(\hbar\omega = 0) + \frac{B(Q)}{\pi}\frac{\Gamma(Q)}{(\hbar\omega)^2 + \Gamma(Q)^2} \tag{1}$$

It consists of an elastic term represented by a $\delta-$function at zero energy transfer with an amplitude $A(Q)$ and a Lorentzian function with amplitude $B(Q)$ and width $\Gamma(Q)$. The former may incorporate a part of ions not moving at all or slower than the time window of the spectrometer whereas the Lorentzian is expected to describe the incoherent dynamics of the Na ions. At small Q-vectors, the fit delivered only a small amplitude of 10 % or less for the elastic amplitude A relative to the total amplitude $(A + B)$. Therefore, A was constrained to zero for the small Q-range up to about 1 Å^{-1}. The Q-range was restricted to the Q-vectors not influenced by the strong Debye-Scherrer line, which prevented a reasonable fit.

At small Q vectors, the fitted linewidth Γ is proportional to DQ^2, the macroscopically expected behavior for diffusion. The proportionality constant D is the self-diffusion coefficient for translational diffusion on long distances. This process is catalyzed by thermal energy and the diffusion constant D should follow an Arrhenius law. For a better understanding of the diffusion mechanism, the evolution of $\Gamma(Q)$ is evaluated using a jump diffusion model. The Chudley Elliott model is based on the assumption of instantaneous jumps over a distance l between sites after resting a time τ and predicts the following Q-dependence for the linewidth in the case of isotropic averaging [16]:

$$\Gamma(Q) = \frac{\hbar}{\tau}(1 - \frac{\sin(Ql)}{Ql}) \tag{2}$$

This model has the correct Q^2 dependence of Γ at small wavevectors. The respective self-diffusion coefficient D is related to the jump length l and the residence time τ according to $D = l^2/(6\ \tau)$.

Spectra for the momentum transfer $Q = 0.96$ Å^{-1} are shown in Fig. 2 for several temperatures. The chosen model can fully describe the lineshape and there is apparently no need for the application of a more complicated model function. Clearly visible is the broadening of the spectra. There is a distinct change with rising temperature even though the change between $T = 1153$ K and $T = 1193$ K is not dramatic. From the fits a Q-dependent linewidth $\Gamma(Q)$, the half width at half maximum of the Lorentzian, is obtained. Fig. 3 shows the results for four temperatures. The lines depict the fits with the Chudley-Elliott model. The fit results for the jump lengths l and the diffusion coefficients D are given in table 1.

	l [Å]	D [10^{-7}cm^2/s]
$T = 1033$ K	3.4 ± 0.1	0.68 ± 0.05
$T = 1073$ K	3.3 ± 0.2	1.2 ± 0.1
$T = 1113$ K	3.5 ± 0.1	2.3 ± 0.1
$T = 1153$ K	3.7 ± 0.1	3.8 ± 0.2
$T = 1193$ K	4.3 ± 0.1	9.2 ± 0.4
$T = 1233$ K	4.7 ± 0.3	16.0 ± 1.8

Table 1
The fit results for the jump length l and the diffusion coefficient D are presented.

The jump length l for the temperatures up to $T = 1153$ K shows a good accord with the distance between the Na position inside an octahedron (Na^{VI}) and a position between them (Na^{VIII}), which is 3.4 Å. This most probable

jump event has also been concluded from molecular dynamics simulations [12]. At higher temperature beyond the transition at $T = 1153\ K$ further jump processes must be taken into account. Jumps to wider distances can be supposed, e.g. from octahedra to octahedra or within the chains between the octahedra. The set-in of dynamical disorder, observed in our previous experiment with larger energy resolution [14], would suggest that more jump possibilities are possible at higher temperature.

In Fig. 4 the diffusion coefficients are plotted over the inverse temperature in a logarithmic scale. The two lines are fits with an Arrhenius law. For both temperature ranges a nearly linear decay suggests that the jump diffusion process follows an Arrhenius law with a single activation energy. For the temperature range above $T = 1153$ K we obtain an activation energy of 195 ± 13 kJ/mol and at the lower temperatures 147 ± 8 kJ/mol. Landon and Ubbelohde derived from their conductivity measurements activation energies of 213 kJ/mol for the temperatures above $T = 1153$ K and 117 kJ/mol for the temperature range between $T = 850$ K and $T = 1140$ K [9]. This agreement supports the conclusion that the main process contributing to the electrical conductivity below the transition temperature is provided by the sodium ion diffusion.

Using a Nernst-Einstein equation the ion diffusion coefficient D can be related to the electrical conductivity σ:

$$\sigma = \frac{e^2 z_{Na}^2}{k_B T} n_{Na} c_{Na} D \tag{3}$$

with e being the electron charge, n_{Na} the sodium particle density, k_B Boltzmann's constant and c_{Na} is the fraction of mobile sodium ions. A mass density of cryolite of $\rho = 2.95$ g/cm^3 was used. As mobile species we only consider the Na ions with charge $z_{Na} = 1$ and $c_{Na} = 1$. Al and F ions are assumed to have negligible contributions to the conductivity.

Fig. 5 shows the derived conductivity values. There is a surprisingly good agreement between the values derived from the sodium diffusion compared with the macroscopic conductivity values. A similar good accord for sodium ion diffusion in sodium silicate glass was already observed some time ago [17]. From this one can conclude that up to the transition temperature at $T = 1153$ K mainly sodium ions contribute to the electrical conductivity. The assumption that all sodium ions are involved in the relevant temperature range ($c_{Na} = 1$) seems to be valid from the good agreement with the electrical conductivity. This concurs also with our earlier assumption in the data analysis that the elastic contribution, at least at small Q-vectors, is negligible.

Above the transition temperature the derived values fail to describe the conductivity in full account. Also the step-like increase is only marginally ex-

pressed. Obviously further diffusion processes must set in to describe completely the conductivity at higher temperatures. In our previous work we already identified two fast processes above $T = 1153$ K, which might be responsible for the increase in the conductivity [14]. One of these processes might involve fluorine diffusion of broken octahedra, a supposition put forward already some time ago [9]. This additional ionic contribution could solve the puzzling question what is responsible for the second step-like increase of the electrical conductivity.

Conclusions

A quasielastic neutron scattering experiment on cryolite at elevated temperature has been performed to study diffusion processes on nanosecond time scales. For cryolite the quasielastic scattering intensity at small momentum transfer values is governed mainly by the sodium ions. This fact allows us to deduce the jump diffusion behavior of the sodium ions. The movements can be described well by a jump diffusion model and results in jumps between the six coordinated position and the eight coordinated sites. Crossing the high temperature transition in the electrical conductivity the jump length increases and indicates more possibilities for jumps over wider distances. The diffusion process follows an Arrhenius law with activation energies in good agreement with values derived from macroscopic conductivity measurements.

Acknowledgment

Sandro Jahn was supported by DFG grant no. JA 1469/4-1.

References

[1] S. Hull, Rep. Prog. Phys. **67** (2004) 1233.

[2] M. O'Keefe, J.-O. Bovin, Science **206** (1979) 599.

[3] C. Ridou, M. Rousseau, B. Pernot, J. Bouillot, J. Phys. C: Solid State Phys. **19** (1986) 4847.

[4] G. W. Watson, S. C. Parker, A. Wall, J. Phys.: Condens. Matter **4** (1992) 2097.

[5] D. Z. Demetriou, C. R. A. Catlow, A. V. Chadwick, G. J. McIntyre, I. Abrahams, Solid State Ionics **176** (2005) 1571.

[6] E. G. Steward, H. P. Rooksby, Acta Cryst. **6** (1953) 49.

[7] Q. Zhou, B. J. Kennedy, J. Sol. State Chem. **177** (2004) 654.

[8] H. Yang, S. Ghose, D. M. Hatch, Phys. Chem. Minerals **19** (1993) 528.

[9] G. J. Landon, A. R. Ubbelohde, Proc. Roy. Soc. Lond. **240** (1957) 160.

[10] D. R. Spearing, J. F. Stebbins, I. Farnan, Phys. Chem. Minerals **21** (1994) 373.

[11] M. Kotecha, S. Chaudhuri, C. P. Grey, L. Frydman, J. Am. Chem. Soc. **127** (2005) 16701.

[12] L. Foy, P. A. Madden, J. Phys. Chem. B **110** (2006) 15302.

[13] E. W. Dewing, Metall. Mat. Trans. B **28** (1997) 1095.

[14] S. Jahn, J. Ollivier, F. Demmel, Solid State Ionics **179** (2008) 1957.

[15] B. Frick, M.A. Gonzalez, Physica B **301** (2001) 8.

[16] R. Hempelmann, Quasielastic neutron scattering and solid state diffusion, Clarendon Press, Oxford, (2000) p120.

[17] R. Hempelmann, C.J. Carlile, D. Bayer, C. Kaps, Zeitschrift für Physik B **95** (1994) 94.

Figures

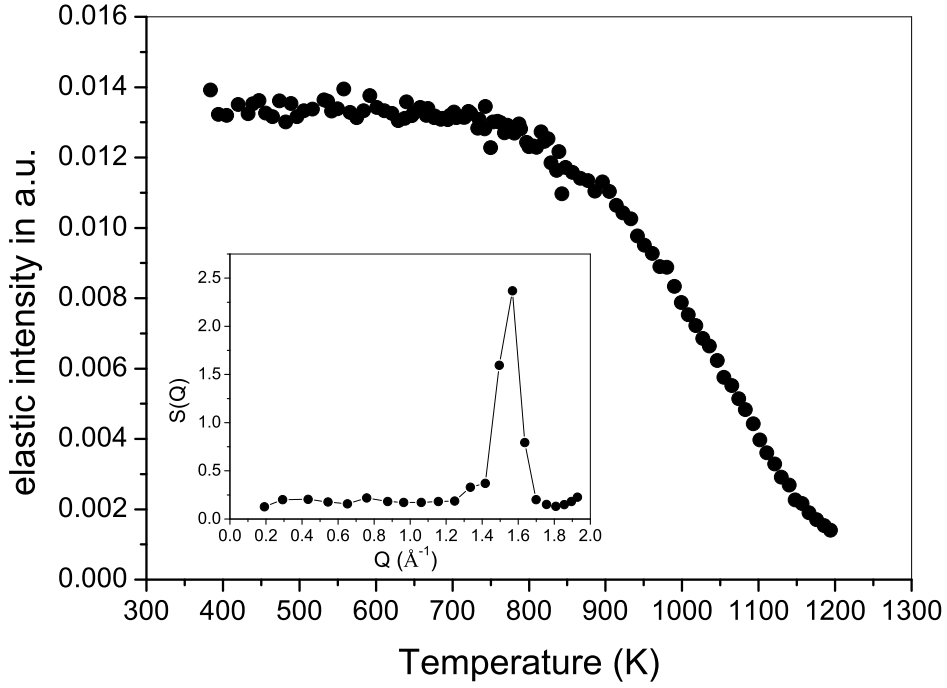

Fig. 1. The elastic intensity from a momentum transfer of $Q = 0.65$ Å^{-1} is shown over temperature. Around $T = 850$ K a decrease of intensity sets in when the sample dynamics is faster than the instrument resolution. In the inset $S(Q)$ derived from an integration over the measured energy range is plotted for $T = 1073$ K.

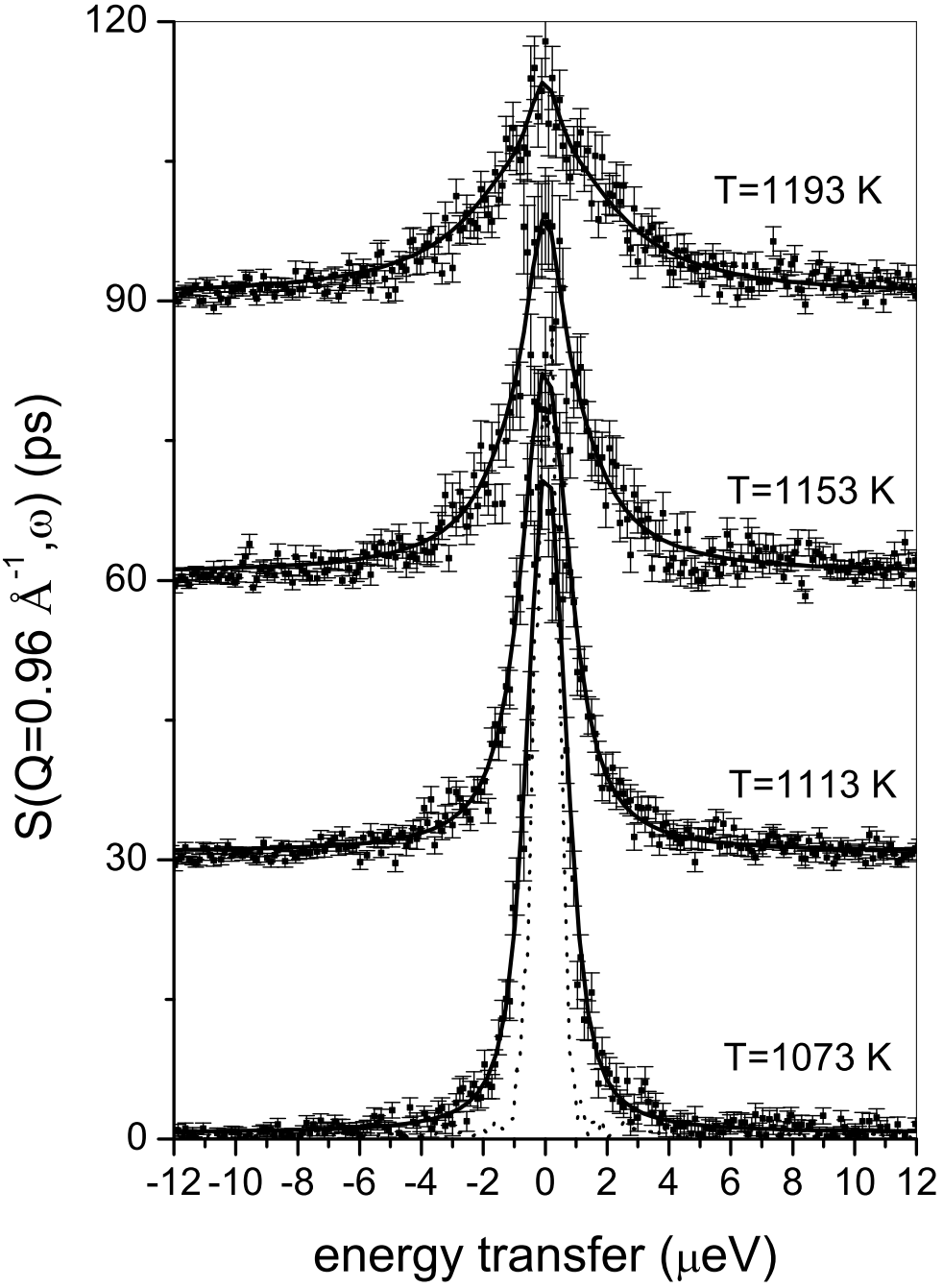

Fig. 2. Several spectra of a single detector at $Q = 0.96$ Å^{-1} are depicted. For clarity they are vertically shifted. All spectra are shown with the resulting fit model. As a dashed line the resolution function is included in the plot for the lowest temperature.

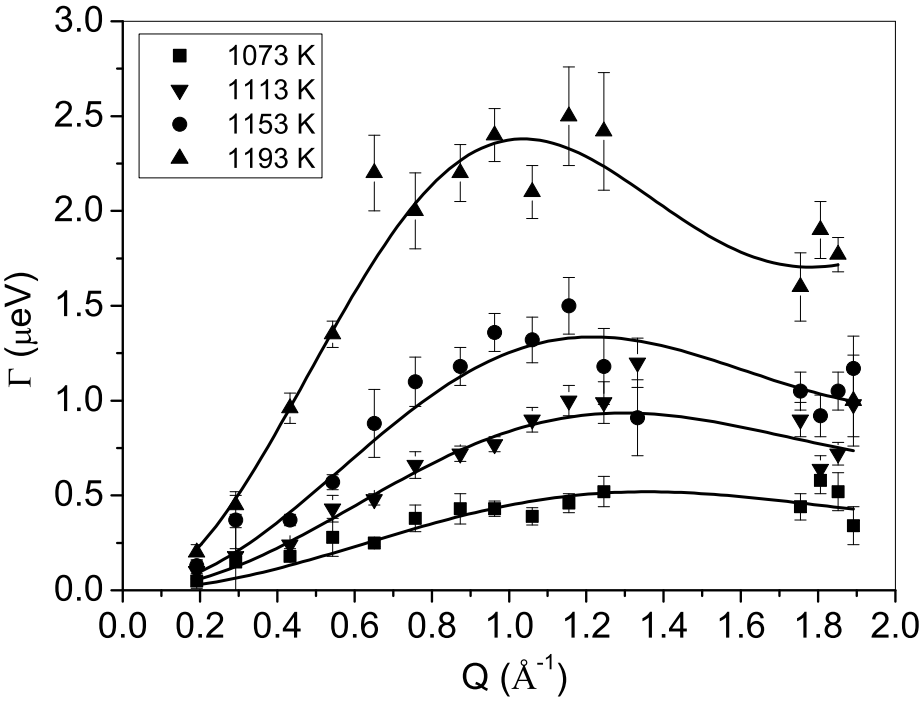

Fig. 3. The figure shows the resulting line width $\Gamma(Q)$ from the fit procedure for four temperatures. The detectors have been fitted individually. The lines depict fits with the Chudley-Elliot jump diffusion model.

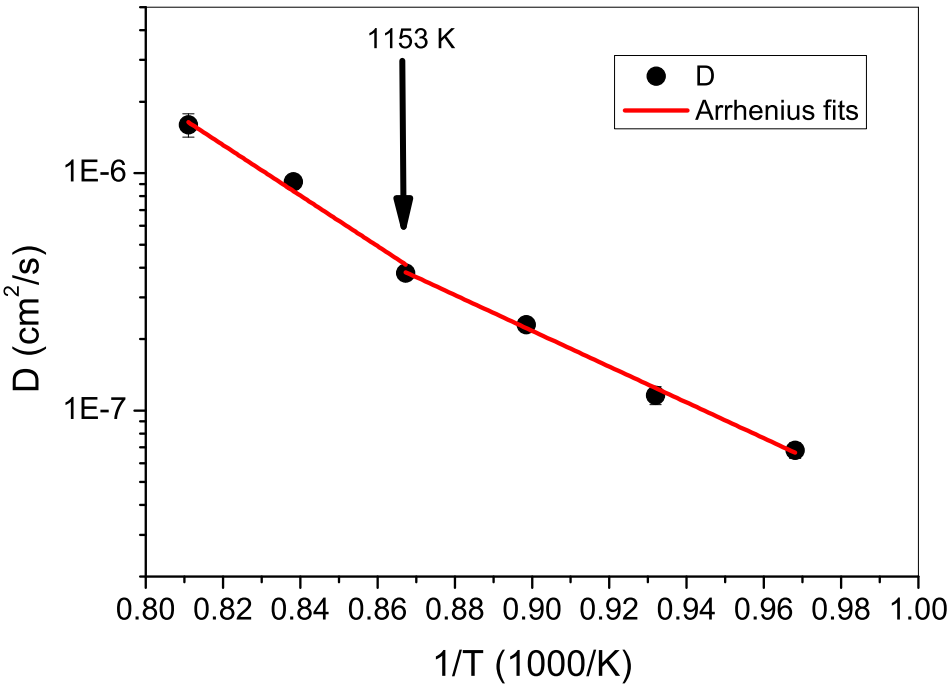

Fig. 4. The derived diffusion coefficients (circles) are shown in a logarithmic scale against the inverse temperature. Two linear fits according to an Arrhenius law are included as lines. The transition temperature where an increase in the electrical conductivity occurs is indicated with an arrow.

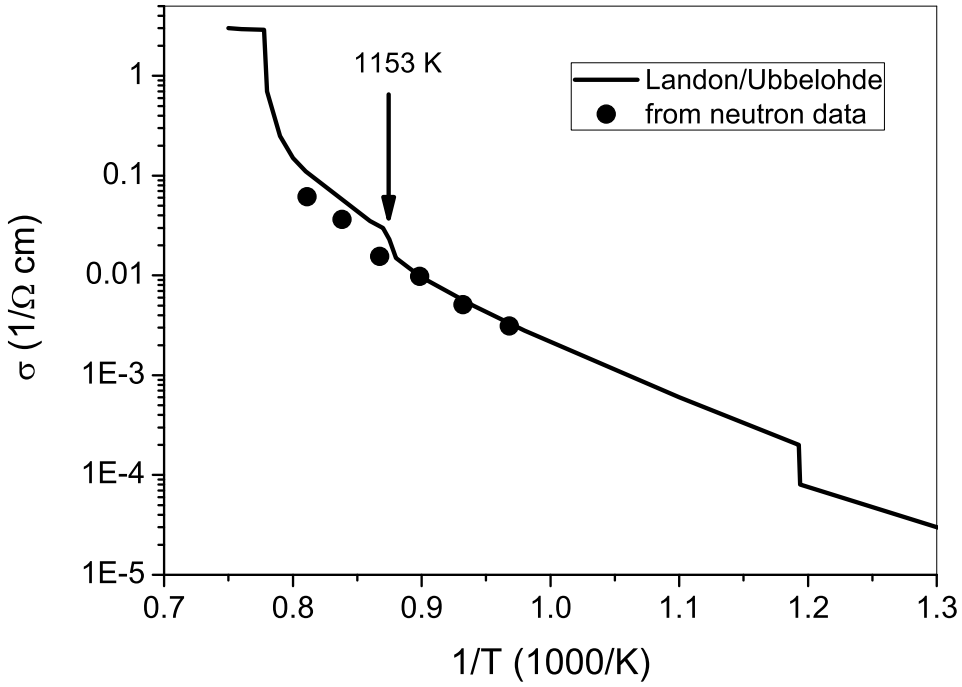

Fig. 5. The electrical conductivity σ derived from the diffusion coefficients (circles) is depicted in a logarithmic scale against the inverse temperature. Included as a line are the conductivity values from Landon and Ubbelohde [9].